

Electrostatic interaction of oppositely charged double layers

A. Flores-Amado

Departamento de Ciencias Básicas, Escuela de Tecnologías de Información y Electrónica, ITESM, Vía atlixcayotl 2301, Reserva Territorial Atlixcayotl 72800, Puebla, Puebla México.

M. Hernández-Contreras

Departamento de Física, Centro de Investigación y Estudios Avanzados del Instituto Politécnico Nacional, Apartado Postal 14-740, México D.F., México.

Recibido el 11 de febrero de 2011; aceptado el 12 de mayo de 2011

We determined with anisotropic hypernetted chain theory the effective pressure and counterion excess of two oppositely charged surfaces immersed in an electrolyte solution. These thermodynamic properties are enhanced in surfaces with evenly smeared surface charges with respect to those containing confined mobile charges. For low surface charges and moderate reservoir salt concentration ions are expelled from the slit between the planes. Depletion arises from ionic charge positional correlations. Its effect was determined through the number of excess of counterions which displays a negative value in the range of low surface charge density. However, a Poisson-Boltzmann calculation lead to positive definite counterion's excess due to its lack of ionic correlations.

Keywords: Electrolyte; double layers; liquid theory; primitive model; colloids.

Determinamos con la teoría cadena hipertejida anisotrópica la presión efectiva y el exceso de contraiones de dos superficies con cargas opuestas inmersas en un electrolito. Estas propiedades termodinámicas se incrementan en superficies con una distribución de carga uniforme que con respecto a aquellas que contienen cargas confinadas discretas y móviles. Para baja densidades superficiales de carga, y concentraciones moderadas de sal en bulto, los iones son expelidos del espacio entre los planos. La reducción de iones se origina por la correlación posicional entre las cargas. Y su efecto fue determinado con el número de contraiones por exceso el cual adquiere valores negativos para bajas densidades de carga superficial. Sin embargo la determinación del exceso de contraiones con la ecuación de Poisson-Boltzmann conduce a valores positivos debido a que ignora las correlaciones iónicas.

Descriptores: Electrolito; dobles capa; teoría de líquido; modelo primitivo; coloides.

PACS: 61.20.Qg; 82.70.Dd; 68.37.-d; 68.15.+e

1. Introduction

In recent years has grown much interest on the effective electrostatic interaction between oppositely planar charged surfaces in aqueous electrolyte solutions [1–5]. Since, it is considered to be an important mechanism that regulates self-assembly of cationic lipid-DNA complexes [6], attachment of biopolymer to cell membrane surface [7], and stability of colloidal suspensions [8]. Most of the theoretical studies by other authors on this system has been conducted by using the Poisson-Boltzmann (PB) theory [1, 2, 9]. Its investigation within mean field theory using 1:1 reservoir electrolyte solutions, lead to the conclusion that equally strength and oppositely charged surfaces are always attractive [10]. And asymmetrically charged planes can either attract or repel as function of the magnitude of surface charge and distance of separation [10]. Yet, repulsion of asymmetrically charged surfaces has been demonstrated experimentally with the atomic force microscope in multivalent electrolytes [3] and confirmed through Monte Carlo simulations [11].

The effective force between the surfaces is comprised of the osmotic pressure due to the reservoir solution, steric and direct electrostatic ion interactions, the short range van der Waals attractive force and the counterion release force. Wagner *et al* [6] determined with osmotic stress techniques that a major mechanism of DNA and lipids self-assembly is driven by the large amount of released counterions from the macro-

molecular species. Thus, the system total free energy is lowered, and the counterions, which were previously confined between the surfaces, are carried out into the bulk solution when the macromolecules surfaces approach each other. The contribution of the counterion release mechanism to the force of two oppositely charged surfaces having a smooth distribution of surface charges was determined numerically from PB theory by Maier-Koll *et al* [1], and comprehensive scaling relations for this property were provided by Safran [9]. Whereas the mean field study of the more general case of asymmetrically charged membranes was performed by Ben Yaakov *et al* [2]. However, real interacting surfaces such as biological membranes have lateral inhomogeneous charge distributions which induces positional density correlations. In the present manuscript we investigated with the use of the anisotropic hypernetted chain (AHNC) theory the total pressure and counterion release due to ion-ion correlations and discrete surface charge distribution. The model system is made of two similarly charged planes of opposite sign in high monovalent saline solutions and with low up to moderate surface charge. We find important differences between mean field and liquid theory which appear at high salt content and low surface charge. Hypernetted chain theory predicts depletion of ions from the slit between the surfaces for low charged plates. Depletion originates from pair ionic correlations that are not taken into account by mean field theory. Correlated density fluctuations arise from hard core and

electrostatic pair direct interactions. Thus, the resulting total counterion and coion concentrations in the slit may become much lower than their bulk saline values. On the other hand, the net pressure between the plates as predicted from AHNC is larger for a smooth density of surface charge than for surfaces having discrete mobile charges.

1.1. Model system and theory

Consider the system consisting of two surfaces with equal magnitude of surface charge $|\sigma|$ and of opposite sign separated the mean distance L by an 1:1 electrolyte in water of dielectric constant $\epsilon = 78.5$. The surfaces have the same dielectric constant as the continuous solvent. In the aqueous phase all ions have the same hydrated diameter $d = 4.25 \text{ \AA}$, therefore, the source field of an ion of species i at a distance r_{3D} is

$$u_i(r_{3D}) = \begin{cases} \frac{q_i}{\epsilon r_{3D}}, & r_{3D} > d \\ \infty, & r_{3D} < d, \end{cases} \quad (1)$$

where it has been included a hard core to avoid overlapping between the spheres and $r_{3D} = \sqrt{r^2 + z^2}$. $q_i = ev_i$ is the charge on sphere i , with $v_i = \pm 1$ being its valence, and e being the electronic charge. r is the radial distance on one surface from the ion to the origin of coordinates. For the case of surfaces bearing discrete charges we consider that each plate has a liquidlike equilibrium distribution of these same sized spheres. We shall not consider neither image charge effects nor the negligible weak van der Waals interactions. At thermal equilibrium the microstructure of the system is obtained from the Ornstein-Zernike equation [12]

$$h_{ij}(r, z_1, z_2) = c_{ij}(r, z_1, z_2) + \sum_\gamma \int dr dz_3 c_{i\gamma}(r, z_1, z_3) n^\gamma(z_3) h_{\gamma j}(r, z_3, z_2), \quad (2)$$

where $h_{ij} = g_{ij} - 1$ and c_{ij} are the total and direct correlation functions respectively, which are obtained self-consistently by the closure relation

$$g_{ij}(r, z_1, z_2) = \exp[h_{ij}(r, z_1, z_2) - c_{ij}(r, z_1, z_2) - \beta u_i(r_{3D}) q_j]. \quad (3)$$

g_{ij} is the pair correlation function. $\beta = 1/k_B T$, and k_B is the Boltzmann's constant and $T = 298 \text{ K}$ is the room temperature. The profile density of ions in the normal direction to the surfaces is determined from [13, 14]

$$n^i(z_1) = \frac{\exp[\beta \mu^i]}{\Lambda_i^3} \exp \left[-\beta q_i \psi(z_1) - \sum_j \int dr dz_2 n^j(z_2) \times \left(\frac{1}{2} h_{ij}^2(r, z_1, z_2) - c_{ij}(r, z_1, z_2) - \beta u_i(r, z_1, z_2) q_j \right) \right] + \frac{1}{2} [h_{ij}(0, z_1, z_1) - c_{ij}(0, z_1, z_1)], \quad (4)$$

where μ^i is the ion's chemical potential that in thermodynamic equilibrium reaches a constant value, while $\Lambda_i \equiv \Lambda$ is its thermal wave length, which is assumed to be the same for all ionic species. In the above equation

$$q_i \psi(z_1) = -4\pi \frac{q_i}{\epsilon} \sigma \left[z_1 - \frac{L}{2} \right] - 2\pi \frac{q_i}{\epsilon} \sum_j \int dz_2 |z_1 - z_2| n^j(z_2) q_j, \quad (5)$$

where $\psi(z_1)$ is the average electric field in the electrolyte phase at position z_1 [13]. We obtained converged solution of Eq. (2) self-consistently with the use of Eqs. (3)-(5) and using a cut off for the long range tail in h_{ij} and c_{ij} that originates from the Coulomb potential [12] (see Appendix). In all our numerical results for AHNC theory, we imposed the overall electroneutrality in the system

$$\int_{z_{\min}}^{z_{\max}} dz [+en^+(z) - en^-(z)] + \sigma - |\sigma| = 0, \quad (6)$$

which allows for the exact match of the different ion's chemical potentials that result from the ionic equilibrium with the reservoir electrolyte, thus, $\mu^+ = \mu_{\pm}^{\text{bulk}} + \chi$ and $\mu^- = \mu_{\pm}^{\text{bulk}} - \chi$ with $\text{Exp}[\mu_{\pm}^{\text{bulk}}] = n_0 \Lambda^3 \gamma_{\pm}$ and γ_{\pm} is the mean activity coefficient corresponding to the concentration n_0 of electrolyte in the bulk solution. The constant χ is obtained self-consistently from the above Eq. (6).

At mean field level, we have taken into account finite ionic size effects by using the Poisson-Boltzmann's equation, Ref. 15

$$\nabla^2 \psi(z) = -\frac{4\pi}{\epsilon} [+en^+(z) - en^-(z)], \quad (7)$$

where the ion's local concentrations are given by

$$n^{\mp}(z) = \frac{n_0 e^{\pm \beta e \psi(z)}}{1 - 2n_0 d^3 + 2n_0 d^3 \cosh(\beta e \psi(z))}. \quad (8)$$

All ions are restricted to reach the distance of closest approach $z_{\min} = d/2$ and $z_{\max} = L - d/2$ from the plates.

From Eqs. (4) and (8) the contact (cont) values of the volume distribution of ions $n_{\text{cont}}^{\mp}(z_{\min})$ are obtained. Therefore, the total (tot) pressure between the walls can be written as

$$P_{\text{tot}} = P_{\text{slit}} - P_{\text{bulk}}, \quad (9)$$

with $P_{\text{slit}} = k_B T [n_{\text{cont}}^+ + n_{\text{cont}}^-] - \frac{\sigma^2}{2\epsilon\epsilon_0}$ from the contact value theorem [16], and the osmotic pressure due to the electrolyte solution $P_{\text{bulk}} = k_B T \phi [n_0^+ + n_0^-]$, where ϕ is the bulk osmotic coefficient associated with the ionic bulk density correlations included in the general AHNC framework, meanwhile in mean field theory $\phi = 1$, and $n_0^{\mp} = n_0$ are the bulk densities of both species of ions. With ϵ_0 the permittivity of vacuum. The excess of counterion release (number of ions in the slit minus their bulk values) is given by

$$N = A \int_{z_{\min}}^{z_{\max}} dz [n^+(z) + n^-(z) - 2n_0]. \quad (10)$$

with A the area element.

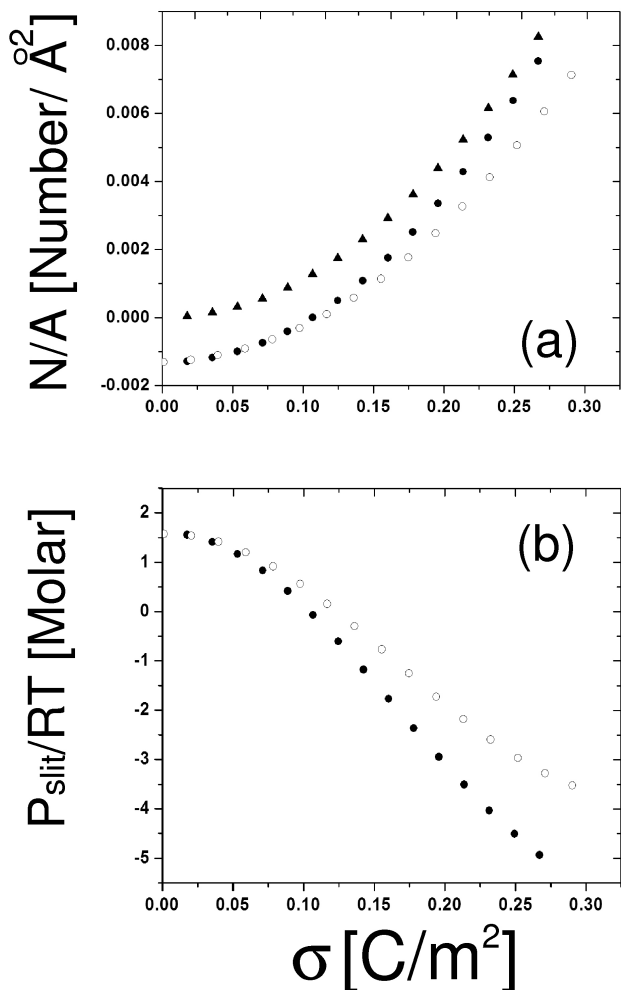


FIGURE 1. (a) calculated excess of counterions N/A as a function of surface charge density σ . Predictions using liquid theory; symbol \circ for discrete, and \bullet smooth surface charge respectively, and mean field result \blacktriangle for case of smooth surface charge only. System; restricted primitive model of 1:1 electrolyte at 1 M concentration between two infinite flat walls separated 9 \AA . Figure (b) are the liquid theory predictions of slit pressure P_{slit}/RT versus surface charge density σ for \circ discrete, and \bullet smooth surface charge, respectively.

2. Results

We considered two model systems; a smeared out, and discrete charges with liquid like structure, on surfaces. Figure 1 depicts the results obtained from AHNC for the two cases with $n_0 = 1.0$ M of 1:1 reservoir electrolyte solution. At this concentration $\gamma_{\pm} = 0.656$. We kept fixed the plates separation to $L = 9$ \AA and varied the surface charge density in the range $0 \leq \sigma \leq 0.3$ C/m^2 . Therefore all thermodynamic properties; $n^{\mp}(z)$, P_{tot} , and N/A were calculated as functions of σ in order to capture their most general behavior for each model studied on this same range of σ . Figure 1a is the plot of the excess of counterions N/A in units of number of particles per Angstrom square. We have included in this

picture also the PB prediction for this property, black filled triangle \blacktriangle , as it is more clear to see its magnitude difference with respect to liquid theory result. And Fig. 1b yields the slit pressure P_{slit} in Molar units versus surface charge. We can observe that only at very low surface charges ($\sigma < .05$ C/m^2) both models coincide and the case of smooth surface charge predicts a larger strength of surface's attractive interaction than the discrete surface charge case.

With an opposite behavior for the monotonously increasing counterion's excess function. Such functional relationship of the pressure and counterion excess as a function of surface charge prevails down to lower salt concentrations too (0.1 M, $\gamma_{\pm} = 0.778$). The PB result for N/A yields the same trends as observed above for the more concentrated case, that is, $N/A > 0$ for all surface charge density (not depicted). However its comparison with liquid theory values becomes less relevant as the concentration of salt is diminished. For instance, at 1M of electrolyte the largest relative difference between mean field and AHNC is 0.00128 $\text{Number}/\text{\AA}^2$, whereas at 0.1 M it has dropped to just 7.26×10^{-5} $\text{Number}/\text{\AA}^2$. Thus, both theories coincide in their predictions on this structural property at low surface charge. There are three distinct regions where $N/A < 0, = 0, > 0$ versus σ , which depends in the difference in magnitudes of

$$A \int_{Z_{\min}}^{Z_{\max}} (n^- + n^+) dz$$

and $A[Z_{\min} - Z_{\max}]2n_0$ in Eq. 10. The result $N/A = 0$ corresponds to the largest possible counterion release from the surfaces and therefore their concentration between the plates is the same as in the bulk. Similarly for the slit pressure, its three distinct regions where $P_{\text{slit}} < 0, = 0, > 0$ are given by

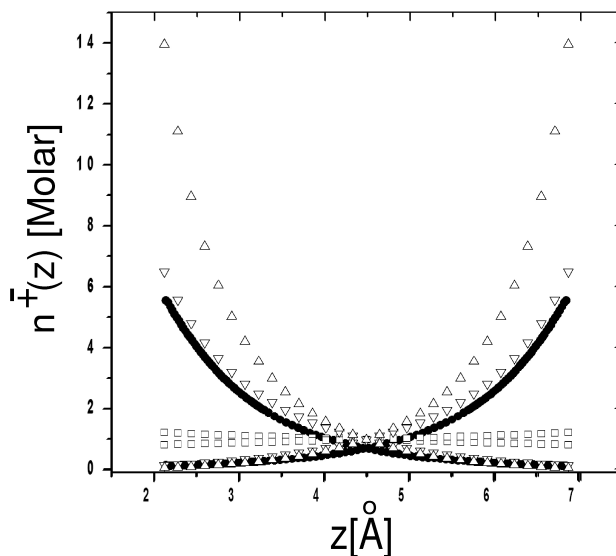


FIGURE 2. Calculated profile concentrations of ions between the two walls with smooth surface charge; mean field results are the symbols Δ , ∇ , \square , for $\sigma = 0.256, 0.178, 0.0178$ C/m^2 , respectively. AHNC result corresponds to \bullet symbol with $\sigma = 0.16019$ C/m^2 . Other system parameters as in Fig. 1.

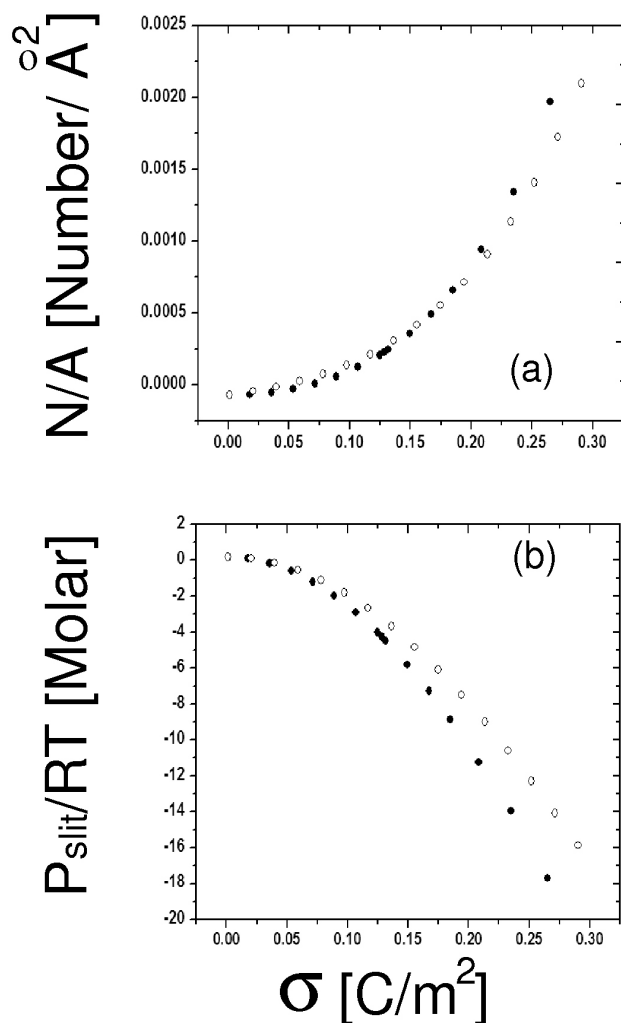


FIGURE 3. Liquid theory prediction of excess of counterions (a) and slit pressure (b) as a function of surface charge for discrete \circ , and smooth \bullet density of surface charge. Wall's separation is 9 Å and salt concentration 0.1 M.

the relative differences in magnitudes of the terms $k_B T(n_{\text{cont}}^+ + n_{\text{cont}}^-)$ and $-\sigma^2/2\epsilon\epsilon_0$. Thus, for increasing surface charge σ , we can observe that there is a correspondence in the general trends between the slit pressure and excess of counterions. Note that the point where the slit pressure turns into negative is roughly the same as for the counterions excess function. Namely, N/A as a function of σ is negative from zero up to the value of $\sigma \approx 0.1$ C/m² after which it turns on positive values. The region where N/A is negative means that there is a depletion of both counterions and coions between the two surfaces for low strength of surface charges. Therefore, the total concentration of ions in the slit turns out to be lower than in the case of bulk solution, namely

$$A \int_{Z_{\min}}^{Z_{\max}} (n^- + n^+) dz < A[Z_{\min} - Z_{\max}]2n_0.$$

This is an important effect that has also been observed in the context of 1:1 electrolytes confined between dielectric hard

flat neutral surfaces in aqueous solvent due to image charges on the walls [17]. Where it was found there appears depletion of ions from the slit for various surface separations. However, in our case depletion of ions results from correlations in core and charge density fluctuations taken into account in AHNC theory. Which it is not present in PB theory due to its lack of such an effect and therefore doesn't predict depletion of ions as can be seen in Fig. 1a (black triangle symbol) for the smooth surface charge model system. Figure 2 is a plot of four profile distributions of ions obtained from the mean field equation 8, for the three surface charges $\sigma=0.256$, 0.178, 0.0178 C/m² (open triangle \triangle , open triangle down ∇ , and open square \square , respectively). And the black filled circle \bullet is the AHNC profile distribution of ions obtained at $\sigma = 0.16019$ C/m². A common feature of the three mean field ion's density profiles is that they predict a bulk concentration of 1.0 M at the middle of the slit $z = 4.5$ Å. Whereas, due to the depletion effect predicted by liquid theory, the ion's profile yields a lower bulk concentration on the order of 0.7 M for $\sigma = 0.16019$ C/m², see Fig. 2.

Due to this breakdown of mean field the predicted slit pressure turns out to be also different from the AHNC results, since the calculated mean field contact values n_{cont}^{\pm} yield also of different magnitudes with respect to liquid theory. Figure 3 is the plot of N/A and P_{slit} versus σ calculated using liquid theory for the lowest electrolyte concentration we considered 0.1 M, while the distance between the surfaces was kept fixed to 9 Å. We find that P_{slit} has a similar trend as in the more concentrated case above. It is larger when σ is smooth than in the discrete surface charge case. However, the property N/A remains approximately equal as calculated from the two model systems in a wider range of surface charges, from low up to moderate values, that is $\sigma \leq 0.2$ C/m². Finally, Fig. 4

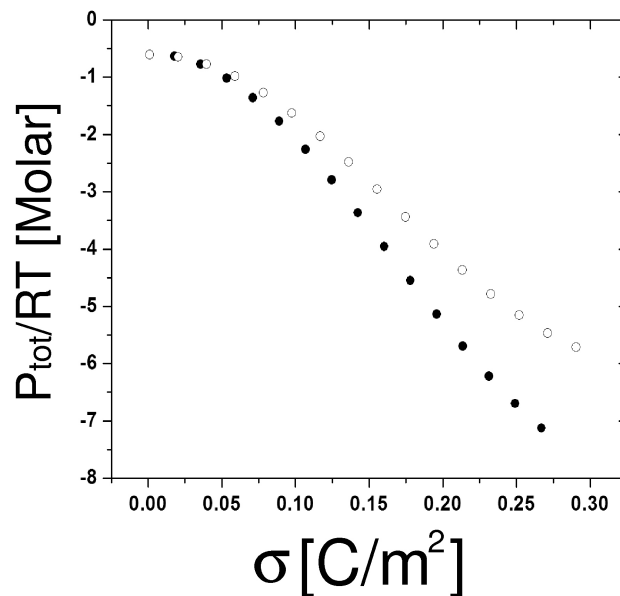


FIGURE 4. AHNC prediction of total pressure between the two walls for discrete \circ , and smooth \bullet density of surface charge σ . Same system parameters as in Fig. 1, and $\phi = 1.094$.

depicts the total AHNC pressure between the surfaces given by Eq. 9 for the two model systems. It is attractive in all of the range of surface charge considered. Being of larger strength for the case of evenly smearing of charges on the surfaces than in the discrete surface charges case.

3. Conclusions

We determined with the hypernetted chain liquid theory the counterion excess and pressure between two flat oppositely charged surfaces bearing either, an evenly smooth, or discrete density. We used as intervening electrolyte the restricted primitive model. When the surface pose a smooth charge density the counterion excess and pressure properties enhance their magnitudes with respect to the case when the confined charges are discrete and formed by mobile ions with a thermodynamic structure of a liquid like model. Another conclusion is that liquid theory predicts depletion of those ions that reside in the slab between the oppositely charged planes, and hence their concentration becomes smaller, at low surface charge, than in the reservoir solution. An effect that is confirmed by the appearance of negative values on the counterion excess function. In addition, and for comparison, we treated this model system, in the case of smooth surface density only, with mean field theory. The Poisson-Boltzmann's equation lack of ionic correlations, in contrast to the AHNC result, leads to positive values on the excess counterion function for all charge density.

Acknowledgments

This work was supported by CONACyT Grant # 48794-F, México.

Appendix

Using the Hankel transforms for the radial dependence

$$f(k) = 2\pi \int_0^{\infty} f(r) J_0(kr) r dr,$$

with inverse

$$f(r) = (1/2\pi) \int_0^{\infty} f(k) J_0(kr) k dk,$$

Eq. (2) becomes

$$h_{ij}(k, z_1, z_2) = c_{ij}(k, z_1, z_2) + \sum_{\gamma} \int dz_3 c_{i\gamma}(k, z_1, z_3) n^{\gamma} h_{\gamma j}(k, z_3, z_2). \quad (1)$$

For the numerical solution of this equation, the z coordinate is discretized into 122 layers between the surfaces. Each layer has a width Δz_m giving a two-dimensional number density per layer, and for species i , $\rho_i^{(m)} \approx \Delta z_m n_i(z^{(m)})$. It is assigned a set of layers to each ionic species through the dependence $i = i(m)$. Also, we can define the independent of i quantity $\rho^{(m)}/\Delta z_m \approx n_{i(m)}(z^{(m)})$. Similarly for the correlation functions we have $f^{(mn)}(k) = f_{i(m)j(n)}(k, z^m, z^n)$. Therefore, the Ornstein-Zernike equation (OZ) in matrix form is $\mathbf{H}(\mathbf{k}) = \mathbf{C}(\mathbf{k}) + \mathbf{H}(\mathbf{k})\mathbf{N}\mathbf{C}(\mathbf{k})$ where \mathbf{H} and \mathbf{C} are matrices of order $m \times n$, and $\{\mathbf{N}\} = \{n^{(m)}\delta_{mn}\}$ a diagonal matrix. δ_{mn} is the Kronecker's delta. The previous matrix form of the OZ equation has the solution $\mathbf{H}(\mathbf{k}) = (\mathbf{I} - \mathbf{C}(\mathbf{k})\mathbf{N})^{-1}\mathbf{C}(\mathbf{k})$, with \mathbf{I} the unit square matrix. Cut of the long range tail of $\mathbf{C}(\mathbf{k})$ is defined through the short range functions c_{ij}^s ,

$$c_{ij}(k, z_i, z_j) = c_{ij}^s(k, z_i, z_j) - q_i q_j / 2\epsilon\epsilon_0 k.$$

Now using the identity matrix

$$(\mathbf{M} - \mathbf{xy}^T)^{-1} = \mathbf{M}^{-1} + \mathbf{M}^{-1}\mathbf{xy}^T\mathbf{M}^{-1} / (1 - \mathbf{y}^T\mathbf{M}^{-1}\mathbf{x}),$$

where \mathbf{x} and \mathbf{y} are column matrices, T means matrix transpose. \mathbf{M} a square matrix. And defining $\mathbf{M} = \mathbf{I} - \mathbf{C}^s\mathbf{N}$, with $\mathbf{x} = \mathbf{q} = \{\mathbf{q}^m\} = \{\mathbf{q}_{i(m)}\}$, $\mathbf{y} = -\mathbf{q}^T\mathbf{N}/2\epsilon\epsilon_0 k$, it yields the solution of the OZ equation

$$\mathbf{H}(\mathbf{k}) = (\mathbf{I} - \mathbf{C}^s\mathbf{N})^{-1}\mathbf{C}^s - \frac{(\mathbf{I} - \mathbf{C}^s\mathbf{N})^{-1}\mathbf{q}\mathbf{q}^T(\mathbf{I} - \mathbf{N}\mathbf{C}^s)^{-1}}{[(k + \mathbf{q}^T\mathbf{N}(\mathbf{I} - \mathbf{C}^s\mathbf{N})^{-1}\mathbf{q}/2\epsilon\epsilon_0)]2\epsilon\epsilon_0}.$$

We used 300 mesh points in the lateral coordinate r .

1. A.A. Meier-Koll, C.C. Fleck, and H.H. von Grünberg, *J. Phys. Condens. Matter* **16** (2004) 6041.
2. D. ben Yakoov, Y. Burak, D. Andelman, and S.A. Safran, *Europhys. Lett.* **79** (2007) 48002.
3. K. Besteman, A.G. Sevenberger, H.A. Heering, and S.G. Lemay, *Phys. Rev. Lett.* **93** (2004) 170802.
4. U. Raviv, P. Laurat, and J. Klein, *J. Chem. Phys.* **116** (2002) 5167.
5. I. Popa, P. Sinha, M. Finessi, P. Maroni, G. Papastavrou, and M. Bokovec, *Phys. Rev. Lett.* **104** (2010) 228301.
6. K. Wagner, D. Harries, S. May, V. Kahl, J.O. Radler, and A. Ben-Shaul, *Langmuir* **16** (2000) 303.
7. C. Fleck and H.H. von Grünberg, *Phys. Rev. E* **63** (2001) 061804.
8. L. Sjöström, T. and Åkesson, *J. Colloid Interface Sci.* **181** (1996) 645.

9. S.A. Safran, *Europhys. Lett.* **69** (2005) 826.
10. V.A. Parsegian and D. Gingell, *Biophys. J.* **12** (1972) 1192.
11. M. Trulsson, B. Jönsson, T. Åkesson, J. Forsman, and C. Labbez, *Phys. Rev. Lett.* **97** (2006) 068302.
12. J.P. Hansen and I.R. McDonald, *Theory of simple liquids*, (Academic, London, 1986).
13. R. Kjellander and S. Marcelja, *J. Chem. Phys.* **82** (1985) 2122.
14. P.H. Attard, R. Kjellander, and D.J. Mitchell, *J. Chem. Phys.* **89** (1988) 1664.
15. I. Borukhov, D. Andelman, and H. Orland, *Electrochim. Acta* **46** (2000) 221.
16. D. Henderson and L. Blum, *J. Chem. Phys.* **75** (1981) 2025.
17. R. Kjellander and S. Marcelja, *Chem. Phys. Lett.* **142** (1987) 485.